

Synthesis and structure of the new oxide fluoride $\text{Ba}_2\text{ZrO}_3\text{F}_2 \cdot x\text{H}_2\text{O}$ ($x \approx 0.5$)

Peter R. Slater^{*a} and Richard K. B. Gover^b

^aDepartment of Chemistry, School of Physics and Chemistry, University of Surrey, Guildford, Surrey, UK GU2 5XH. E-mail: p.slater@surrey.ac.uk; Tel: 01483 876847; Fax: 01483 876851

^bDepartment of Chemistry, University of Durham, Science Laboratories, South Road, Durham, UK DH1 3LE

Received 1st May 2001, Accepted 18th May 2001

First published as an Advance Article on the web 3rd July 2001

In this paper we report the synthesis of the new oxide fluoride $\text{Ba}_2\text{ZrO}_3\text{F}_2 \cdot x\text{H}_2\text{O}$ ($x \approx 0.5$) from the reaction of Ba_2ZrO_4 with NH_4F or transition metal difluorides (CuF_2 , ZnF_2) at low temperature (250 °C). The fluorination reaction represents a substitution of 1 oxygen by 2 fluorines, thus increasing the anion content and resulting in a large expansion of the unit cell in the c direction (tetragonal, $I4/mmm$, $a = b = 4.1721(3)$, $c = 16.376(2)$ Å). Powder neutron diffraction studies have shown that the material has a K_2NiF_4 -type structure similar to the precursor Ba_2ZrO_4 , with the extra anions occupying interstitial sites within the rock salt layers, which accounts for the large expansion in the unit cell along the c direction. The anion content determined from the neutron diffraction data refinement is higher than expected for the simple oxide fluoride $\text{Ba}_2\text{ZrO}_3\text{F}_2$. This is attributed to the additional incorporation of water as OH groups, which is supported by TGA and high temperature XRD studies. On heating to 500 °C a mass loss consistent with the loss of 0.5 moles of H_2O was observed along with a reduction in the cell parameters to $a = b = 4.180(6)$, $c = 15.45(3)$ Å for the dehydrated phase. On heating to higher temperatures (> 500 °C) decomposition to BaF_2 and the perovskite phase BaZrO_3 was observed.

These results and preliminary work showing the successful fluorination of related phases demonstrate both the versatility of these low temperature fluorination routes, and the ready ability of the K_2NiF_4 structure to incorporate extra anions.

Introduction

In recent years there has been a resurgence of interest in the preparation and study of inorganic oxide fluorides with perovskite related structures. High temperature synthesis and structural studies of a range of materials, *e.g.* BaScO_2F_1 , have been reported by Needs and Weller.^{1–4} However, in most cases, synthesis by high temperature solid state reaction is not possible, due to the stability of the simple fluoride starting materials relative to the intended products. Research has therefore been directed at overcoming this problem, and two general strategies have thus been employed, high pressure synthesis and low temperature synthesis. High pressure synthesis has been successful in the preparation of new superconducting copper oxide fluorides,^{5,6} but requires expensive equipment and the sample sizes are quite small. The use of low temperature synthesis routes is therefore to be desired, and such routes have been successfully applied to cuprate systems. Studies by Al Mamouri *et al.* showed that the low temperature (220 °C) reaction of Sr_2CuO_3 with F_2 gas gives the superconducting oxide fluoride $\text{Sr}_2\text{CuO}_2\text{F}_{2+\delta}$.⁷ Further work showed that other fluorinating agents, NH_4F , MF_2 ($\text{M} = \text{Cu}$, Ni , Zn), XeF_2 could also be employed to prepare this oxide fluoride.^{8–10} These low temperature routes have been subsequently demonstrated to be suitable for the fluorination of a wide range of cuprate materials,^{11–15} and recently Greaves *et al.* and Case *et al.* have demonstrated the successful synthesis of new manganese and iron based oxide fluorides.^{16,17}

In order to investigate the possible widespread applicability of the low temperature fluorination methods, we decided to examine the possible fluorination of the phase Ba_2ZrO_4 . This

phase has the K_2NiF_4 structure consisting of perovskite BaZrO_3 units separated by rock salt BaO blocks, and this structure type was chosen as successful fluorination has been achieved in previous studies of related cuprate, ferrate, and manganate materials.^{7,12,14,16,17} Unlike these latter systems, however, there is no possibility for a change in oxidation state for Ba_2ZrO_4 , and so the importance or otherwise of having a transition metal with variable oxidation state on the fluorination reaction could be assessed. The fluorination proved to be successful and led to the synthesis of the new oxide fluoride $\text{Ba}_2\text{ZrO}_3\text{F}_2 \cdot x\text{H}_2\text{O}$, which is reported here. We also report the determination of the structure of this phase from powder neutron diffraction studies.

Experimental

High purity BaCO_3 and ZrO_2 were used to prepare the precursor phase Ba_2ZrO_4 . The oxide and carbonate were intimately mixed in the correct stoichiometry and heated to 1050 °C for 12 hours in air, before regrinding and reheating at the same temperature for a further 12 hours.

Ba_2ZrO_4 readily absorbs H_2O from the air, and so prior to fluorination was dried at 900 °C. Two fluorination routes were employed, reaction with NH_4F (method 1), and reaction with MF_2 ($\text{M} = \text{Cu}$, Zn) (method 2). For each method the fluorination was performed on approximately 0.5 g samples of Ba_2ZrO_4 . It was found that single phase fluorinated samples could be prepared for an $\text{F} : \text{Ba}_2\text{ZrO}_4$ ratio of approximately 2 : 1.

In the case of method 1, the dried Ba_2ZrO_4 was ground with

2.5 mole equivalent of NH_4F (representing a 25% excess over the stoichiometric reaction). The resulting mixture was then held at 90°C for 2 hours, before raising the temperature to 250°C for 15 hours. The mixture was then reground and reheated at the same temperature for a further 15 hours.

Method 2 involved the addition of anhydrous CuF_2 or ZnF_2 (1.1 mole; 10% excess) to the Ba_2ZrO_4 ; the mixture was ground, then held at 90°C for 2 hours before raising the temperature to 250°C for 15 hours. As for method 1, the mixture was reground and reheated at 250°C for a further 15 hours.

Characterisation

X-Ray diffraction

The products were characterised by powder X-ray diffraction (Cu $\text{K}\alpha$ radiation Seifert XRD 3003TT diffractometer) with both methods giving similar results. After fluorination a large shift in the peaks associated with the c axis was observed (Fig. 1). Refinement of the cell parameters indicated that the c axis undergoes a very large expansion ($\approx 22\%$), while a small contraction along a, b was observed (Ba_2ZrO_4 , $a=b=4.181(1)$, $c=13.459(4)$ Å; fluorinated phase, $a=b=4.1721(3)$, $c=16.376(2)$ Å).

High temperature X-ray diffraction data were collected on a Bruker d8 advance diffractometer (Cu $\text{K}\alpha 1$ only) equipped with an Mbraun position sensitive detector. All high temperature measurements were performed using an Anton Parr HTK1200 furnace attachment.

Since there is no possibility, in the samples studied, for there to be an increase in metal oxidation state, it is reasonable to assume that the fluorination is a substitution one, with 2 F atoms replacing one O atom to give a general formula $\text{A}_2\text{MO}_{4-x}\text{F}_{2x}$ ($x \approx 1$). The actual fluorine content was determined by fluorine analysis (ion selective electrode), as outlined below.

Fluorine analysis

Prior to measurements being made, the electrode was calibrated using freshly prepared solutions containing known concentrations of NaF. The sample solution was then prepared as follows: ca. 0.020 g of sample was dissolved in 5 cm^3 of 1 M HCl, to which was added 145 cm^3 of distilled water followed by 50 cm^3 of a pH ca. 5.3 total ionic strength buffer (TISAB) solution. The fluorine content of the sample was then determined from the electrode reading of the solution using the NaF calibration graph. No noticeable residual fluorinating agent (NH_4F , CuF_2 , ZnF_2) was present in any of the samples analyzed. Potential errors in the analysis are due to the presence of any $\text{SrF}_2/\text{BaF}_2$ impurities, although in the samples analyzed the levels of these impurities were small according to XRD.

Assuming a composition of $\text{Ba}_2\text{ZrO}_3\text{F}_2$, the fluorine analysis should give a fluorine content of 8.4%. The actual value determined was 8.8%, in good agreement with this.

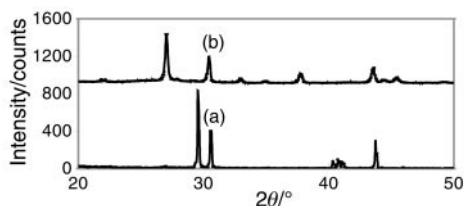


Fig. 1 X-Ray diffraction pattern for (a) Ba_2ZrO_4 and (b) sample fluorinated with NH_4F .

Structure determination and discussion

One problem with method 2 is the CuO/ZnO impurity originating from the decomposition of the fluorinating agent $\text{CuF}_2/\text{ZnF}_2$. Therefore, for the structural characterization a sample prepared using method 1 (NH_4F) was examined to avoid the problem of impurities in the structure refinement.

Data was collected on the GEMeral Materials Diffractometer (GEM), ISIS, Rutherford Appleton Laboratory. As this data was collected during commissioning experiments, it was necessary to collect using the 90° detectors banks rather than the backscattering banks. The data was collected for approximately 2 hours on a 0.5 g sample. Rietveld refinement was performed using the GSAS suite of programs.¹⁸

Structure refinement was based on the space group $I4/mmm$, as observed for a range of K_2NiF_4 systems. A number of other space groups were also investigated but these tended to give worse fits or the refinements were unstable.

The anion content of $\text{Ba}_2\text{ZrO}_3\text{F}_2$ is 5 compared to 4 for the simple K_2NiF_4 structure, and the excess anions were put in interstitial positions, O3/F3 (0, 0.5, 0.25), between the rock salt layers (Fig. 2), as observed in structural refinements of related systems containing excess interstitial anions. Due to the similar neutron scattering factors of oxygen and fluorine, it is not possible to distinguish which sites are occupied by oxygen and which fluorine. We presume, however, that the fluorine preferentially occupies the interstitial and apical anion positions, as supported by modelling studies of related systems.^{19,20} Therefore these positions have been labelled O3/F3 and O2/F2 respectively, with the equatorial positions as O1 (Fig. 2). In order to confirm this, computer modelling studies are required for this system.

Initially the site occupancies of the O1 and O2/F2 positions were entered as 1.0, while the O3/F3 occupancy was entered as 0.5 to give the total anion content of 5. Towards the end of the refinement, these occupancies were allowed to vary, and although the O1 site occupancy remained at 1.0, the O2/F2 site showed evidence of reduced occupancy, while the O3/F3 site showed evidence of increased occupancy. The presence of these interstitial anions accounts for the large expansion in the unit cell c axis on fluorination.

A high temperature factor was observed for the O1 site, with a particularly large value for U_{33} (Table 1). Attempts were therefore made to allow for displacement of O1 off site along the z direction. This, however, led to unstable refinements and so in the final refinement, the O1 position was fixed back on the ideal (0,0.5,0) site.

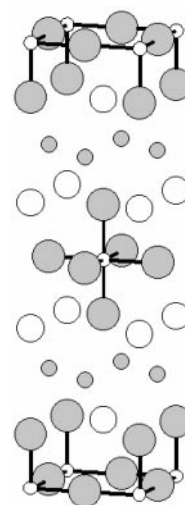


Fig. 2 The structure of $\text{Ba}_2\text{ZrO}_{4-x}\text{F}_{2x}$ (large white spheres = Ba, small white spheres = Zr, large grey spheres = O/F in normal K_2NiF_4 anion sites, small grey spheres = interstitial O/F ions).

Table 1 Refined structural parameters for Ba₂ZrO₃F₂·0.5H₂O^a

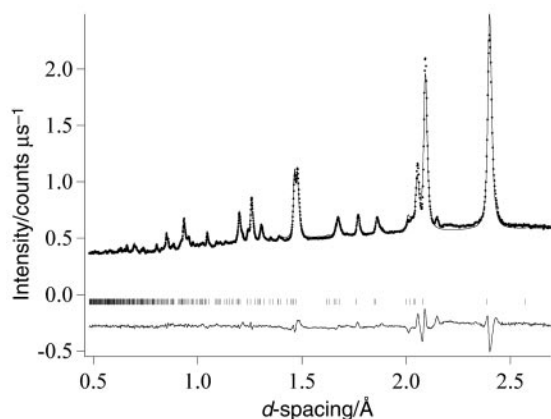
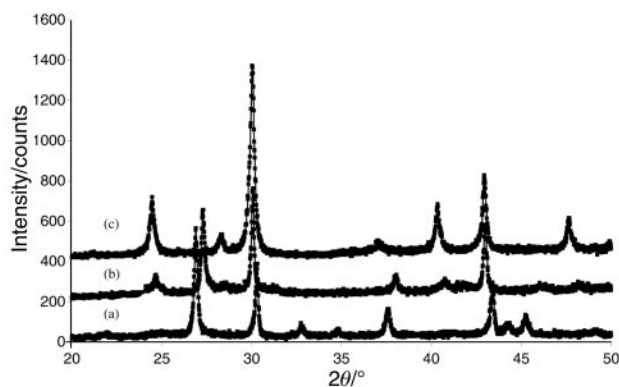
Atom	Site	<i>x</i>	<i>y</i>	<i>z</i>	<i>B</i> /Å ²	Site occ.
Ba	4e	0	0	0.3593(3)	1.29	1.0
Zr	2a	0	0	0	1.01	1.0
O1	4c	0	0.5	0	2.58	1.0
O2/F2	4e	0	0	0.1221(4)	1.11	0.89(2)
O3/F3	4d	0	0.5	0.25	1.25	0.84(2)
		$100 \times U_{11}/\text{Å}^2$	$100 \times U_{22}/\text{Å}^2$	$100 \times U_{33}/\text{Å}^2$		
Ba		0.78(11)	0.78(11)	3.4(4)		
Zr		0.24(8)	0.24(8)	3.35(28)		
O1		1.76 (23)	-0.37(12)	8.43(44)		
O2/F2		1.04(14)	1.04(14)	2.1(4)		
O3/F3		2.59(15)	0.85(15)	-0.40(14)		

^a*U*₁₂, *U*₁₃, *U*₂₃=0. Tetragonal, *I4/mmm*; *a*=*b*=4.1721(3), *c*=16.376(2) Å. *R*_p=2.80, *R*_{wp}=2.79.

Table 2 Selected bond distances for Ba₂ZrO₃F₂·0.5H₂O

Bond	Bond distance/Å
Ba–O1	3.108(4) [× 4]
Ba–O2/F2	2.966(1) [× 4]
Ba–O3/F3	2.749(4) [× 4]
Zr–O1	2.086(1) [× 4]
Zr–O2/F2	2.000(7) [× 2]

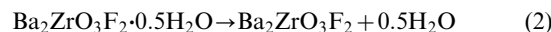
The final refined parameters are given in Table 1, with selected bond distances in Table 2, and the refined neutron diffraction profiles in Fig. 3. From the occupancies of the anion sites, we obtain a composition Ba₂Zr(O,F)_{5.5(1)}. Thus the anion content, at 5.5(1), is higher than the expected value of 5. One possible explanation for the higher anion content is the presence of H₂O incorporated into the interstitial sites as OH groups. In order to check this possibility, the neutron diffraction sample was examined using thermogravimetric analysis (Stanton Redcroft STA780 thermal analyser). Approximately 50 mg of sample was heated in air at 5 °C min⁻¹ up to 500 °C and held for 30 minutes. A 2.0% mass loss was observed, which is consistent with a loss of ≈0.5 moles of H₂O in good agreement with the neutron diffraction data. Therefore the composition of the sample appears in fact to be Ba₂ZrO₃F₂·0.5H₂O (or Ba₂ZrO_{2.5}(OH)F₂ representing the likelihood that H₂O incorporation gives OH anions in the structure). Other support for the presence of H₂O, is the fact that the precursor oxide itself, Ba₂ZrO₄, readily absorbs water to give Ba₂ZrO₄·*x*H₂O.²¹ In addition, the presence of water in the sample is not that surprising, especially when it is considered that water is a byproduct of the

**Fig. 3** Observed, calculated and difference neutron diffraction profiles for Ba₂ZrO₃F₂·0.5H₂O.**Fig. 4** High temperature X-ray diffraction data for Ba₂ZrO₃F₂·0.5H₂O; (a) room temperature, (b) 500 °C, (c) 900 °C.

fluorination reaction with NH₄F, eqn. (1):



High temperature X-ray diffraction data was collected to follow the dehydration and subsequent decomposition process for Ba₂ZrO₃F₂·0.5H₂O and this data is summarised in Fig. 4. By 500 °C, the water has been lost to give Ba₂ZrO₃F₂ which results in a reduction in unit cell volume (*a*=*b*=4.180(6), *c*=15.45(3) Å vs. *a*=4.1721(3), *c*=16.376(2) Å). In particular there is a significant contraction (≈6%) in the *c* axis consistent with the loss of interstitial species, eqn. (2):



If the sample is heated above 500 °C decomposition occurs to give products (BaZrO₃ and BaF₂) in complete agreement with the composition of the initial phase being Ba₂ZrO₃F₂·0.5H₂O, eqn. (3):



On fluorination the coordination sphere of the Ba increases as a result of the interstitial anions. If these interstitial positions were completely filled, 12 coordination would result. The incomplete occupancy of the interstitial sites and the apical sites means, however that the coordination is lower. It is interesting to note the long bond distances between Ba and the normal anion positions (O1, O2/F2), with the distances to the interstitial anions (O3/F3) being significantly shorter (Table 2). A high temperature factor is observed for O1 (particularly for *U*₃₃) and this may be due to displacements of some of the oxygen atoms to shorten the long Ba–O1 bond. Indeed it is likely that there is also some tilting/twisting of the octahedra,

which would account for the high thermal parameters, although the complexities of this system mean that this is impossible to model. All in all, however, there appears to be significant changes in the coordination around the Ba sites. In contrast, the Zr coordination is maintained at 6 coordinate, although there are some vacancies in the apical sites, meaning that there must be some 5 coordinate Zr. Zr–O/F bond distances are in the region 2.0–2.09 Å (Table 2). It is therefore mainly the Ba environment which changes on fluorination.

We have also performed preliminary studies to examine the versatility of these low temperature routes for the fluorination of K₂NiF₄ type oxides, and have succeeded in fluorinating a wide range of systems, e.g. Sr₂TiO₄, Ba₂SnO₄, Ba₂HfO₄, Ba₂ScO₃F, LaSrMO₄ (M = Ga, Fe, Co). This work is ongoing with optimisation of synthesis conditions underway and powder neutron diffraction studies planned. Further studies investigating the fluorination of Ba₂ZrO₄ have shown evidence for at least two other fluorinated phases, one with higher fluorine content and one with lower fluorine content. Work is ongoing to optimise the synthesis conditions to achieve single phase samples of these materials.

In summary it has been shown that the low temperature fluorination (using NH₄F, CuF₂, ZnF₂) of the K₂NiF₄ type phase Ba₂ZrO₄ can be used to prepare the new oxide fluoride Ba₂ZrO₃F₂·0.5H₂O. These results demonstrate the versatility and widespread applicability of these low temperature fluorination routes, and so these methods have great potential for use in the synthesis of a wide range of novel inorganic oxide fluoride systems. The results also show the ready ability of the K₂NiF₄ structure to incorporate extra interstitial anions (located in sites between the rock salt layers) at low temperatures.

Acknowledgements

We would like to thank EPSRC for the provision of neutron diffraction time. We would also like to thank P. Radaelli and A.C. Hannon for help with the collection of the neutron diffraction data.

We would also like to thank J.S.O. Evans (University of Durham) for the provision of high temperature X-ray diffraction facilities.

References

- 1 R. L. Needs and M. T. Weller, *J. Chem. Soc., Chem. Commun.*, 1995, 353.
- 2 R. L. Needs and M. T. Weller, *J. Chem. Soc., Dalton Trans.*, 1995, 3015.
- 3 R. L. Needs, M. T. Weller, U. Scheler and R. K. Harris, *J. Mater. Chem.*, 1996, **6**, 1219.
- 4 R. L. Needs and M. T. Weller, *J. Solid State Chem.*, 1998, **139**, 422.
- 5 T. Kawahima, Y. Matsui and E. Takayama-Muromachi, *Physica C*, 1996, **257**, 313.
- 6 M. Isobe, J. Q. Li, Y. Matsui, F. Izumi, Y. Kanke and E. Takayama-Muromachi, *Physica C*, 1996, **269**, 5.
- 7 M. Al-Mamouri, P. P. Edwards, C. Greaves and M. Slaski, *Nature (London)*, 1994, **369**, 382.
- 8 P. R. Slater, P. P. Edwards, C. Greaves, I. Gameson, J. P. Hodges, M. G. Francesconi, M. Al-Mamouri and M. Slaski, *Physica C*, 1995, **241**, 151.
- 9 P. R. Slater, J. P. Hodges, M. G. Francesconi, P. P. Edwards, C. Greaves, I. Gameson and M. Slaski, *Physica C*, 1995, **253**, 26.
- 10 E. I. Ardashnikova, S. V. Lubarsky, D. I. Denisenko, R. V. Shpanchenko, E. V. Antipov and G. Van Tendeloo, *Physica C*, 1995, **253**, 259.
- 11 J. L. Yang, J. K. Liang, G. H. Rao, Y. L. Qin, Y. Shi and W. H. Tang, *Physica C*, 1996, **270**, 35.
- 12 P. R. Slater, J. P. Hodges, M. G. Francesconi, C. Greaves and M. Slaski, *J. Mater. Chem.*, 1997, **7**, 2077.
- 13 E. V. Antipov, S. N. Putilin, R. V. Shpanchenko, V. A. Alyoshin, M. G. Rozova, A. M. Abakumov, D. A. Mikhailova, A. M. Balagurov, O. Lebedev and G. Van Tendeloo, *Physica C*, 1997, **282**, 61.
- 14 A. M. Abakumov, J. Hadermann, G. Van Tendeloo, R. V. Shpanchenko, P. N. Oleinikov and E. V. Antipov, *J. Solid State Chem.*, 1999, **142**, 440.
- 15 G. B. Peacock, I. Gameson, M. Slaski, J. J. Capponi and P. P. Edwards, *Physica C*, 1997, **289**, 153.
- 16 C. Greaves, J. L. Kissick, M. G. Francesconi, L. D. Aikens and L. J. Gillie, *J. Mater. Chem.*, 1999, **9**, 111.
- 17 G. S. Case, A. L. Hector, W. Levason, R. L. Needs, M. F. Thomas and M. T. Weller, *J. Mater. Chem.*, 1999, **9**, 2821.
- 18 A. C. Larsen and R. B. Von Dreele, Los Alamos Laboratory report, NO-LA-U-86-748, Los Alamos, NM, 2000.
- 19 M. S. Islam and S. D'Arco, *Chem. Commun.*, 1996, 2291.
- 20 J. P. Hill, N. L. Allan and W. C. Mackrodt, *Chem. Commun.*, 1996, 2703.
- 21 R. V. Shpanchenko, E. V. Antipov and L. M. Kovba, *Zh. Neorg. Khim.*, 1993, **38**, 599.